Plant Physiology Preview. Published on January 14, 2014, as DOI:10.1104/pp.113.233395

Running title: Modulation of terpenoid metabolism by chalcone isomerase

Corresponding author: Gregg A. Howe

Department of Energy–Plant Research Laboratory, Michigan State University, East Lansing, Michigan 48824

Phone Number: +1 5173555159

Email: howeg@msu.edu

Research Area: Biochemistry and Metabolism

The flavonoid biosynthetic enzyme chalcone isomerase modulates terpenoid production in glandular trichomes of tomato

Jin-Ho Kang[a], John McRoberts[a], Feng Shi[b], Javier E. Moreno[a], A. Daniel Jones[b,c], and Gregg A. Howe[a,c,*]

[a] Department of Energy-Plant Research Laboratory, Michigan State University, East Lansing, Michigan 48824

[b] Department of Chemistry, Michigan State University, East Lansing, Michigan 48824

[c] Department of Biochemistry and Molecular Biology, Michigan State University, East Lansing, Michigan 48824

One-sentence summary: An isoform of chalcone isomerase coordinates flavonoid and terpenoid metabolic pathways in glandular trichomes of tomato.

Footnotes:

This research was supported in part by a grant from the National Science Foundation (DBI-0604336). Support for J-H.K. and generation of transgenic tomato lines was provided by the Chemical Sciences, Geosciences and Biosciences Division, Office of Basic Energy Sciences, Office of Science, U.S. Department of Energy (grant DE–FG02–91ER20021).

Corresponding Author: Gregg A. Howe; Email howeg@msu.edu; Fax: (517) 353-9168

ABSTRACT

Flavonoids and terpenoids are derived from distinct metabolic pathways but nevertheless serve complementary roles in mediating plant interactions with the environment. Here, we show that glandular trichomes of the *anthocyanin free* (*af*) mutant of cultivated tomato (*Solanum lycopersicum*) fail to accumulate both flavonoids and terpenoids. This pleiotropic metabolic deficiency was associated with loss of resistance to native populations of coleopteran herbivores under field conditions. We demonstrate that *Af* encodes an isoform (*Sl*CHI1) of the flavonoid biosynthetic enzyme chalcone isomerase (CHI), which catalyzes the conversion of naringenin chalcone to naringenin and is strictly required for flavonoid production in multiple tissues of tomato. Expression of the wild-type *SlCHI1* gene from its native promoter complemented the anthocyanin deficiency in *af*. Unexpectedly, the *SlCHI1* transgene also complemented the defect in terpenoid production in glandular trichomes. Our results establish a key role for *Sl*CHI1 in flavonoid production in tomato and reveal a link between CHI1 and terpenoid production. Metabolic coordination of the flavonoid and terpenoid pathways may serve to optimize the function of trichome glands in dynamic environments.

INTRODUCTION

Flavonoids and terpenoids (isoprenoids) comprise two of the largest groups of specialized metabolites in higher plants. They serve myriad and often complementary roles in plant acclimation to changing environmental conditions. For example, flavonoids and terpenoids directly repel attack by insect herbivores and microbial pathogens, and also mediate plant communication with symbiotic bacteria, natural enemies of arthropod herbivores, and parasitic plants (Hirsch et al., 2003; Rasmann et al., 2005). Pigmented flavonoids and volatile terpenes provide visual and olfactory cues, respectively, for attraction of insect pollinators (Dudareva et al., 2006; Grotewold, 2006), and also protect against ultraviolet radiation, elevated temperature and oxidative stress (Li et al., 1993; Sharkey and Singsaas, 1995; Affek and Yakir, 2002). Much of the scientific interest in flavonoids and terpenoids reflects their importance in food quality, nutrition, and human health (Dillard and German, 2000; Middleton et al., 2000; Dixon et al., 2005; Bohlmann and Keeling, 2008).

Flavonoids are synthesized from phenylalanine derivatives generated via the shikimate and phenylpropanoid pathways (Tohge et al., 2013) (Fig. 1). Chalcone synthase (CHS; EC 2.3.1.74) condenses 4-coumaroyl-CoA and malonyl-CoA to form the open-chain flavonoid naringenin chalcone, which is converted to naringenin by chalcone isomerase (CHI; EC 5.5.1.6). Naringenin defines a key branch point for synthesis of several major classes of flavonoids, including flavanones, flavonols, and anthocyanins. Flavonoid biosynthesis is controlled by transcription factors that coordinate the expression of multiple biosynthetic genes in response to environmental and developmental cues (Dixon and Paiva, 1995; Grotewold, 2006; Vogt, 2010). Terpenoids originate from distinct metabolic pathways in which the C5 precursors dimethyl allyl diphosphate (DMAPP) and isopentenyl diphosphate (IPP) are sequentially combined to produce the building blocks for C10 monoterpenes, C15 sesquiterpenes, and higher-molecular-weight derivatives. Plastid-derived terpenoids are synthesized by the methyl-erythritol-phosphate (MEP) pathway (Fig. 1), whereas most extraplastidic terpenoids are produced from the cytosolic mevalonic acid (MVA) pathway (Bohlmann and Keeling, 2008). Relatively little is known about the regulatory mechanisms governing terpenoid biosynthesis in higher plants (Patra et al., 2013).

The terpenoid and flavonoid biosynthetic pathways are supplied with carbon skeletons generated in primary metabolism but, otherwise, are thought to operate independently of one another in most plant tissues (Fig. 1). Recent studies, however, are beginning to uncover

metabolic and regulatory connections between these two major branches of specialized metabolism. For example, DMAPP is used for the synthesis of prenylated flavonoids and other terpenophenolics in glandular trichomes of some plant species (Nagel et al., 2008; Wang et al., 2008; Shen et al., 2012; Voo et al., 2012). There is also evidence that members of the MYB family of transcription factors play a role in coordinating metabolic activity between the flavonoid and terpenoid biosynthetic pathways (Bedon et al., 2010; Ben Zvi et al., 2012).

Glandular trichomes provide an excellent model system in which to study the production of specialized metabolites in a single, experimentally accessible cell type (Wagner, 1991; Lange et al., 2000; Schilmiller et al., 2008; Voo et al., 2012). The type VI glandular trichome of tomato (*Solanum lycopersicum*) is particularly well suited for analysis of flavonoid and terpenoid synthesis, which dominates the metabolic activity of this specialized epidermal structure (Duffey and Isman, 1981; Kennedy, 2003; van Schie et al., 2007; Schilmiller et al., 2010; Kang et al., 2010b). Mutants affected in the chemical composition, morphology and density of type VI glands have provided insight into the biological roles of glandular trichomes in resistance to insect herbivores (Li et al., 2004; Kang et al., 2010a; Kang et al., 2010b; Bleeker et al., 2012). Both the development and biosynthetic capacity of type VI trichomes are responsive to environmental inputs and are regulated in part by the stress hormone jasmonate (Li et al., 2004; Boughton et al., 2005; van Schie et al., 2007; Peiffer et al., 2009; Tian et al., 2012). The mechanisms that coordinate the developmental and metabolic plasticity of glandular trichomes in tomato and other species are largely unknown.

The *anthocyanin free* (*af*) mutant of tomato was identified more than a half-century ago as an x-ray-induced variant that lacks anthocyanin production in all tissues (Burdick, 1958). In contrast to other anthocyanin-deficient mutants of tomato, Rick and co-workers showed that *af* foliage exhibits a lower density of type VI glandular trichomes, reduced emission of leaf volatiles, and increased susceptibility to herbivorous flea beetles (Rick et al., 1976). These pleiotropic phenotypes led to the suggestion that *af* may define a regulatory gene that controls both flavonoid production and trichome development (De Jong et al., 2004), but this hypothesis has remained untested. Here, we demonstrate that *Af* encodes a member (*Sl*CHI1) of the CHI family of enzymes that catalyzes the synthesis of a key branch point intermediate [2(*S*)-naringenin] in the flavonoid pathway. Transgenic complementation experiments showed that *Af*/*CHI1* is required not only for the synthesis of anthocyanins and other flavonoids, but also

plays a role in promoting the accumulation of terpenoids in glandular trichomes. These findings suggest a role for CHI1 in coordinating the developmental plasticity and metabolic activity of an epidermal structure that shields against biotic stress.

RESULTS

The *af* Mutant is Deficient in Flavonoid Accumulation in Type VI Glandular Trichomes

Under growth conditions in which wild-type (WT) plants accumulate relatively high anthocyanin levels, *af* mutant plants lacked visible anthocyanin pigmentation in all tissues, including leaves, stems, and hypocotyls (Fig. 2, A–D). This defect is associated with reduced density of type VI glandular trichomes on leaves, as previously reported (Rick et al., 1976). We found that the density of type VI trichomes on the adaxial surface of *af* leaves (400 ± 54 cm^{-2}) was approximately 30% of that on WT leaves (1379 ± 129 cm^{-2}). Light microscopy and scanning electron microscopy (SEM) confirmed these findings and also showed that the size of type VI glands on *af* leaf and stem tissue is reduced in comparison to WT (Fig. 2, E-F).

Chlorogenic acid (caffeoylquinate) and rutin (quercetin-3-O-rutinoside), which are both derived from 4-coumaroyl-CoA (Fig. 1), are two of the most abundant phenolic compounds in tomato leaves and type VI glands, respectively (Duffey and Isman, 1981; Kang et al., 2010b). To further characterize the effect of *af* on phenolic metabolism, we used liquid chromatography-mass spectrometry (LC-MS) to measure the levels of chlorogenic acid, rutin and other non-volatile secondary metabolites in leaf-dip extracts obtained by brief immersion of excised leaflets into acidified methanol. *af* leaves contained <10% WT levels of rutin and other flavonol derivatives, including kaempferol rhamnoside, a quercetin trisaccharide, and 3-O-methylmyricetin (Fig. 3A). WT and *af* leaves contained similar levels of chlorogenic acid and its precursor, quinic acid, as well as acyl sugars and glycoalkaloids (α-tomatine and dehydrotomatine). Metabolite analyses performed with isolated type VI trichomes confirmed that the mutant produces only trace levels of rutin in gland cells (Fig. 3B). Low levels of acyl sugars were found in type VI extracts from both WT and *af*, whereas chlorogenic acid, quinic acid, and glycoalkaloids were not detected in these extracts (Fig. 3B). These results indicate that *af*, in addition to blocking anthocyanin production in tissues throughout the plant, impairs the flavonoid branch of phenylpropanoid metabolism in type VI trichome glands.

The *af* Mutant Exhibits Increased Susceptibility to Herbivorous Beetles

The defense-related roles of glandular trichome-derived metabolites led us to test whether *af* plants are affected in resistance to native populations of arthropod herbivores. Greenhouse-grown WT and *af* seedlings were transplanted to the field and subsequently monitored for the presence of herbivores and associated leaf damage. Potato flea beetle (*Epitrix cucumeris*) was observed much more frequently on the mutant than on neighboring WT plants (Fig. 4A). Moreover, *af* foliage received more herbivore damage than WT leaves, as determined by counting the number of flea beetle feeding sites (Fig. 4B). We also found that *af* plants were visited by two additional beetle species, Colorado potato beetle (*Leptinotarsa decemlineata*) and blister beetles (*Epicauta funebris*), which were not observed on WT plants (Fig. 4C and D). These results are consistent with previous field studies showing that the *af* mutant is compromised in resistance to native populations of the tobacco flea beetle, *Epitrix hirtipennis* (Rick et al., 1976).

af* is a Null Mutation in *Chalcone Isomerase

The *Af* locus was previously mapped to an interval on chromosome 5 that is defined by the *S. pennellii* introgression line IL5-2 (Tanksley et al., 1992; Eshed and Zamir, 1995). Fine mapping of the locus allowed us to position *Af* to a ~200 kb region flanked by markers SGN-U571424 and CT93 (Fig. 5A). Among the ~31 hypothetical genes in this region were two tandemly duplicated genes predicted to encode the flavonoid pathway enzyme CHI (Fig. 5B). The well-established role of CHI in flavonoid biosynthesis indicated that these genes, which we designated *CHI1* (Solyc05g010320) and *CHI2* (Solyc05g010310), were good candidates for *Af*. Reverse transcription (RT)-PCR analysis showed that *CHI1* transcripts are expressed in both WT and *af* leaves, whereas expression of *CHI2* was not detected in leaves of either genotype (Supplemental Fig. S1). This finding is consistent with publically available gene expression data for *CHI1* and *CHI2* (http://solgenomics.net). Sequencing of WT- and *af*-derived genomic clones containing *CHI2* did not reveal nucleotide polymorphisms at this locus. *CHI1* genomic and cDNA clones isolated from *af*, however, contained a six nucleotide deletion (preceded by a G-to-T transversion) within the last exon. This polymorphism generates a premature stop codon that truncates the C-terminal 18 amino acids of the protein (Fig. 5C).

Based on an x-ray crystal structure of CHI (Jez et al., 2000), the C-terminal truncation of CHI1 in *af* is predicted to affect an α helix (α7) that does not participate directly in enzyme catalysis. We therefore performed experiments to determine whether the mutant form of *Sl*CHI1 is enzymatically active. Histidine-tagged derivatives of WT ($CHI1^{WT}$) and mutant ($CHI1^{af}$) CHI1 were expressed in *E. coli* and purified to homogeneity. The amount of soluble $CHI1^{af}$ recovered from induced *E. coli* cells was low in comparison to $CHI1^{WT}$, and we found that this difference in expression resulted largely from partitioning of $CHI1^{af}$ to the insoluble fraction (Supplemental Fig. S2A and data not shown). *In vitro* assays performed with affinity-purified proteins showed that $CHI1^{WT}$ rapidly metabolizes the substrate naringenin chalcone. In contrast, the activity of $CHI1^{af}$ was not greater than that of control reactions lacking enzyme (Fig. 5D).

We used immunoblot assays to determine whether $CHI1^{af}$ accumulates in the *af* mutant. Polyclonal antibodies raised against $CHI1^{WT}$ reacted strongly and specifically with a single polypeptide in WT leaves (Fig. 5E). The apparent M_r of this protein, which was recovered in both supernatant and pellet fractions of crude leaf extracts, matched the predicted size of CHI1 (24.6 Kd). The anti-CHI1 antibody did not specifically recognize proteins in the soluble or particulate fraction from *af* leaves. Control experiments performed with recombinant enzymes showed that the absence of immunoreactive CHI1 in *af* did not result from failure of the antibody to recognize $CHI1^{af}$ (Supplemental Fig. S2B). These results indicate that the *af* mutation eliminates enzymatic activity of *Sl*CHI1 and also prevents accumulation of the protein *in planta*.

We used chemical and genetic complementation approaches to test whether the *af* mutant is impaired in CHI1-mediated conversion of naringenin chalcone to naringenin. Consistent with a metabolic block at this step, supplementation (through the cut stem) of seedlings with exogenous naringenin led to anthocyanin accumulation in the major veins of naringenin-treated but not mock-treated *af* plants (Fig. 6A). In genetic experiments, we used *Agrobacterium*-mediated transformation to introduce the WT *CHI1* gene, expressed from the native *CHI1* promoter, into the *af* mutant background. We recovered 16 independent primary (T_0) transformants that accumulated anthocyanins in leaf and stem tissue following transfer of explants from tissue culture medium to soil. Four representative anthocyanin-accumulating (AC^+) lines (*CHI1::CHI1*-2, -3, -4, -9) and one anthocyanin-deficient (AC^-) line (*CHI1::CHI1*-20) were selected for further analysis (Fig. 6, B and C). All five of these transgenic lines tested positive by PCR for the presence of the *pCHI1::CHI1* transgene. Western blot analysis confirmed that CHI1 protein

accumulated in the AC^+ lines but not the AC^- line (Fig. 6C). Spectrophotometric assays showed that the level of anthocyanin in the AC^+ lines was >5-fold of that in the *af* parental line, and ranged from 68 to 113% of that in WT leaves. The anthocyanin content of *CH1I::CHI1*-20 was not significantly different from that in leaves of the *af* mutant. These collective findings demonstrate that the anthocyanin deficiency of the *af* mutant results from loss of function of a single CHI isoform, *Sl*CHI1.

*Sl*CHI1 Modulates Terpenoid Production in Type VI Glandular Trichomes

Given the identification of *af* as a *CHI1* mutant, we next addressed the question of why *af* plants lack of the typical aroma of tomato foliage (Rick et al., 1976). Gas chromatography-mass spectrometry (GC-MS) was employed to analyze the volatile composition of WT and *af* leaves and type VI trichomes. Analysis of leaf-dip extracts showed that *af* produces <15% of WT levels of several monoterpenes, including α-pinene, 2-carene, α-phellandrene, α-terpinene, and β-phellandrene (Fig. 7A). The levels of two sesquiterpenes, δ-elemene and β-caryophyllene, were also reduced in *af* leaves. Analyses of extracts from isolated type VI trichome glands, which are the main source of tomato leaf terpenoids (Kang et al., 2010a; Kang et al., 2010b), yielded similar results (Fig. 7B).

To investigate the genetic basis of the terpenoid deficiency in *af* trichomes, we measured the level of β-phellandrene (the major monoterpene) in progeny from a cross between *af* and its parental line (cv Red Cherry). Analysis of the anthocyanin phenotype in both the F_1 and F_2 (260 F2 plants) confirmed that *af* segregates as a monogenic recessive mutation (197 AC^+:63 AC^- plants; χ^2=0.04, *P*=0.8415) and further showed that the AC^+ and AC^- phenotypes within this population are unambiguous (e.g., Fig. 2). The β-phellandrene content in type VI glands of F_1 plants was approximately one-third of that in glands from the WT parent but significantly greater than that of *af* plants (Supplemental Fig. S3A), suggesting that *af* is semidominant with respect to the terpenoid phenotype. Analysis of β-phellandrene levels in leaf-dip extracts from 56 randomly selected F_2 individuals (34 AC^+ and 22 AC^- plants) showed that the amount of β-phellandrene in AC^+ plants was consistently greater than that in AC^- individuals (Supplemental Fig. S3B). The mean level of β-phellandrene in AC^- (*af*/*af*) plants was 30.5% of that in AC^+ (*Af*/-) siblings. This finding establishes a genetic linkage between the anthocyanin and terpenoid phenotypes.

The terpenoid deficiency in *af* trichomes could result from loss of CHI1 function or, alternatively, a secondary mutation closely linked to the *Af* locus. To distinguish between these possibilities, we measured the terpenoid content in leaves of *CHI1::CHI1* transgenic lines described above. The level of the major monoterpene (β-phellandrene) in type VI glands isolated from four independent complemented (AC^+) lines ranged between 39 and 97% of that in WT trichomes (Fig. 8A). Similarly, the level of β-caryophyllene in these lines ranged between 93 and 110% of WT levels (Fig. 8B). In all four complemented lines, terpenoid levels were significantly greater than that in the congenic *af* parent. The terpenoid content of glands isolated from the non-complemented (AC^-) control line (*CHI1::CHI1*-20) was comparable to that in the *af* mutant. Analysis of terpenoid levels in leaf-dip extracts obtained from the same genotypes gave similar results (Supplemental Fig. S4A). These findings indicate that the terpenoid deficiency of *af* leaves is caused by the defect in *CHI1*.

DISCUSSION

Af Encodes a Chalcone Isomerase

Mutations affecting anthocyanin pigmentation have been instrumental not only as markers in classical plant genetics, but also as tools to identify flavonoid biosynthetic genes and associated regulatory loci in many plant species (Grotewold, 2006). Several mutations in tomato cause complete loss of anthocyanin pigments which, depending on environmental conditions, typically accumulate in hypocotyls, stems, abaxial leaf surfaces, and cortical cells at the base of trichomes (von Wettstein-Knowles, 1967). Here, we provide several independent lines of evidence to demonstrate that anthocyanin deficiency in the *af* mutant results from loss-of function of an isoform (CHI1) of CHI. The small deletion identified in the *CHI1* gene from *af* plants abolishes CHI enzymatic activity and also prevents accumulation of CHI1 protein. Transgenic complementation experiments showing that the anthocyanin deficiency is restored by expression of the WT *CHI1* gene from its native promoter showed that the *af* mutation is responsible for the defect in flavonoid production. Consistent with a biochemical role for *Sl*CHI1 in cyclization of naringenin chalcone to the corresponding flavanone (naringenin), exogenous naringenin restored anthocyanin accumulation in vascular tissues of the *af* leaves. A search of the *S. lycopersicum* genome (http://solgenomics.net/) identified seven genes annotated as CHI or CHI-like sequences.

Phylogenetic analyses showed that only two of these, *CHI1* and *CHI2*, are closely related to canonical CHIs that catalyze cyclization of chalcones to tricyclic (*S*) flavanones (Supplemental Fig. S5). The five remaining CHI-like genes in tomato are predicted to encode polypeptides most closely related to non-catalytic CHI-fold family proteins, which bind fatty acid substrates (Ngaki et al., 2012). The apparent lack of *CHI2* expression, together with the strong flavonoid deficiency of the *af* mutant, indicates that CHI1 is the major isoform for flavonoid production in tomato leaves. As expected, we found that *af* plants are deficient in the production of other naringenin-derived metabolites, including rutin and several flavonol glycosides. The *af* mutant should provide a useful genetic tool to assess the physiological roles and nutritional importance of flavonoid production in tomato. Because low levels of some flavonoids (e.g., rutin) were detected in *af* leaves, we cannot exclude the possibility that another CHI isoform plays a minor role in flavonoid biosynthesis, or that naringenin chalcone is converted non-enzymatically to naringenin at very low levels (Bednar and Hadcock, 1988).

Mutations affecting the phenylpropanoid and flavonoid pathways can have pleiotropic effects on plant growth, development and fertility (Taylor and Grotewold, 2005; Peer and Murphy, 2007; Schilmiller et al., 2009). Although *af* abolishes the activity of CHI1 and eliminates anthocyanin production, obvious defects in the growth and development of the mutant were not apparent. This finding is consistent with the view that flavonoids are not essential for normal growth and development of tomato under optimized growth conditions. We did notice, however, that the fruit size of *af* plants was smaller than that of cv Red Cherry, which is the parental line employed for the x-ray mutagenesis used to generate the mutant (Burdick, 1958). This observation raises the possibility that the “WT” line (LA0337; cv Red Cherry) we used for our studies is not isogenic with the *af* accession LA1049. These considerations, together with the fact that the x-ray mutagenesis is likely to have introduced other mutations, highlights the necessity of using genetically complemented lines for comparative analyses of *af*-related phenotypes.

The crystal structure of the functional monomer of CHI from alfalfa and Arabidopsis has provided detailed information about the active site topology of the enzyme, which appears to be highly conserved in a wide range of plant species (Jez et al., 2000; Ngaki et al., 2012). As expected, residues involved in enzyme catalysis and formation of the active site are well conserved in tomato CHI1 (Supplemental Fig. S6). Although the C-terminal α-helix (α7) that is truncated by the *af* mutation does not participate directly in substrate binding or catalysis, it does

form an α-helical segment (helix-turn-helix α6-α7) that bounds the enzyme's active site (Jez et al., 2000; Ngaki et al., 2012). Our results show that this mutation not only abolishes the *in vitro* activity of the enzyme, but also prevents accumulation of the protein in *af* tissues. Accordingly, *af* is a true null mutant with respect to CHI1 function. Our ability to detect *CHI1* transcripts but not the corresponding CHI1 protein in *af* leaves suggests that truncation of α7 destabilizes the protein *in planta*.

Modulation of Terpenoid Production by CHI1

Previous studies showed that *af* plants, unlike several other anthocyanin-deficient mutants tested, are highly susceptible to attack by native populations of insect herbivores (Rick et al., 1976). Of particular interest was the finding that increased susceptibility of *af* plants to insect attack was associated with a "lack of foliage aroma" and a striking reduction in the density of type VI trichomes. Based on the results of genetic co-segregation tests, Rick et al. (1976) concluded that the anthocyanin defect and altered reactivity to herbivore attack is most likely conditioned by a single gene (*af*). Our results confirm and extend these findings in several ways. First, we demonstrate that glandular trichomes from *af* leaves are deficient in mono- and sesquiterpenes that are derived from the MEP and MVA pathways, respectively (Schilmiller et al., 2009; Schilmiller et al., 2010). This pleiotropic metabolic defect explains the lack of leaf volatiles and presumably accounts for the aroma-related phenotype of *af* leaves. We also found that the size and density of type VI glands on *af* leaves is reduced in comparison to WT plants. Under our standard growth conditions, the reduction in trichome density was not as severe as that reported by Rick et al (1976). These differences may reflect plant growth conditions (e.g., light intensity) or plant developmental stage, which can have strong quantitative effects on trichome characteristics. Finally, our field studies performed in East Lansing, MI, like those conducted in Davis, CA (Rick et al., 1976), showed that the *af* mutant is highly susceptible to attack by native populations of flea beetles (*Epitrix* spp). We also observed that other species of herbivorous beetles were more prevalent on *af* compared to WT plants grown in the same test plot. Increased susceptibility to insect herbivores has been demonstrated for other trichome mutants of tomato, including *hairless* (*hl*) and *odorless-2* (*od-2*), which are also deficient in the production of trichome-borne terpenoids (Kang et al., 2010a; Kang et al., 2010b). These collective observations are consistent with the view that tomato leaf volatiles act as repellents of

herbivorous beetles (Rick et al., 1976) and, more generally, highlight the importance of glandular trichomes in mediating tomato-herbivore interactions (Kennedy, 2003; Li et al., 2004; Howe and Jander, 2008; Peiffer et al., 2009; Bleeker et al., 2012).

Given the well-established role of CHI in flavonoid biosynthesis and the distinct nature of flavonoid and terpenoid metabolic pathways, the ability of the WT *CHI1* gene to complement the terpenoid-deficient phenotype of *af* was unexpected. Indeed, the pleiotropic phenotypes of *af* led De Jong et al. (2004) to propose that *af* likely defines a regulatory gene such as *TRANSPARENT TESTA GLABRA1* (*TTG1*), which controls both anthocyanin production and trichome development in Arabidopsis (Walker et al., 1999). There are several hypotheses to explain why loss of CHI1 results in decreased production of terpenoids in type VI glands. For example, a flavonoid pathway intermediate or end product whose synthesis depends on CHI1 may promote, either directly or indirectly, terpenoid production. This idea is consistent with studies showing that flavonoids can modulate gene expression and various hormone responses (Peer and Murphy, 2007; Ringli et al., 2008; Pourcel et al., 2013).

An alternative hypothesis is that accumulation of naringenin chalcone (the substrate of CHI1) or another upstream pathway intermediate inhibits terpenoid production in gland cells. This potential mechanism of metabolic cross-regulation is analogous to the recently discovered role of a MEP pathway intermediate (methylerythritol cyclodiphosphate) in controlling the expression of stress-responsive nuclear genes (Xiao et al., 2012). Naringenin chalcone, like other open-chain flavonoids within the chalcone family, possesses as an electrophilic α,β-unsaturated carbonyl group that contributes to the broad biological activities of chalcones, including inhibition of various biosynthetic and regulatory proteins (Sahu et al., 2012). We speculate that reduced CHI activity in glandular trichomes of the *af* mutant may lead to increased levels of naringenin chalcone, which could potentially react with glutathione to alter cellular redox status, or modify cysteine groups in proteins. In this context, it is noteworthy that naringenin chalcone accumulates in tomato fruit peel, indicating that CHI is a rate-limiting step in flavonol biosynthesis in this tissue (Muir et al., 2001). Similarly, regulation of CHI1 expression in type VI glands by developmental or environmental cues could provide a mechanism to control metabolic flux through both the flavonoid and terpenoid pathways. Measurement of naringenin chalcone levels in type VI glands from WT and mutant lines will provide a critical test of this hypothesis. It is also possible that the regulatory effect of CHI1 on terpenoid production is not dependent on

isomerase activity *per se* but rather on the ability of CHI1 to bind a related small molecule. Interestingly, one of the most highly expressed genes in hop glandular trichomes encodes a CHI-like protein that is inactive as a CHI (Wang et al., 2008).

Our genetic analyses suggested that although *af* is fully recessive with respect to the anthocyanin phenotype, the mutation appears to be semi-dominant with respect to terpenoid production in type VI trichomes. Given our uncertainty about the genetic relationship between *af* and cv Red Cherry (see above), this conclusion awaits confirmation through detailed characterization of genetically complemented *af* lines. Nevertheless, a semi-dominant effect of *af* on terpenoid production would suggest that a single functional allele of *CHI1* is insufficient to meet the metabolic demand for terpenoid production in cells of the trichome gland. Haploinsufficiency in plants often involves multiprotein complexes associated with metabolic processes (Meinke, 2013). Indeed, there is evidence that CHI and other flavonoid biosynthetic enzymes assemble into multiprotein complexes (Burbulis and Winkel-Shirley, 1999). The dual cytosolic/nuclear localization of CHI has also led to the suggestion that CHI-derived compounds may regulate gene expression in Arabidopsis (Saslowsky et al., 2005). These collective studies raise the possibility that CHI1 may modulate terpenoid production through interaction with proteins involved in terpenoid production, or with proteins required for the expression of genes encoding terpenoid biosynthetic enzymes. Given the prevalence of transcription factor binding to exons (Stergachis et al., 2013), we cannot exclude the possibility that the *af* deletion mutation indirectly affects the activity of regulatory proteins that control the expression of terpenoid pathway genes.

Flavonoid and terpenoid biosynthesis dominate the metabolic activity of glandular trichomes in many plant species (Lange et al., 2000; Aziz et al., 2005; Nagel et al., 2008; Wang et al., 2008; Sallaud et al., 2009; Wang et al., 2009; Chatzopoulou et al., 2010; Dai et al., 2010; Schilmiller et al., 2010; McDowell et al., 2011; Bleeker et al., 2012; Tissier, 2012). Although genes encoding many of the respective biosynthetic enzymes have been identified and characterized in detail, it remains to be determined how metabolic flux through these two apparently disparate pathways is coordinated. That such coordination exists is supported by studies showing that emission of phenylpropanoid/flavonoid- and terpenoid-derived components of scent in snapdragon flowers is controlled by similar developmental and environmental (e.g., diurnal) cues (Dudareva et al., 2000; Dudareva et al., 2003). More intriguingly, recent transgenic

studies provide evidence for the existence of transcription factors that promote metabolic flux through both pathways (Bedon et al., 2010; Ben Zvi et al., 2012). Our characterization of pleiotropic metabolic defects in the tomato *af* mutant is consistent with the emerging role of secondary metabolites as lineage-specific signals that coordinate responses to changing environments (Clay et al., 2009; Jander and Clay, 2011; Xiao et al., 2013). Currently, we have no evidence that the *af* mutation impairs terpenoid production in cell types other than type VI glands. It is therefore possible that modulation of terpenoid metabolism by CHI1 reflects a mechanism to coordinate the development and biosynthetic capacity of this specialized defensive structure (Kliebenstein, 2013). The enhanced susceptibility of *af* plants to attack by coleopteran herbivores further suggests that flavonoid-terpenoid cross-regulation impacts species interactions in an ecologically meaningful way (Stam et al., 2013). Future studies are needed to address the mechanisms by which secondary metabolites, or the enzymes that produce them, exert specific effects on seemingly unrelated metabolic pathways.

MATERIALS AND METHODS

Plant Materials and Growth Conditions

Tomato (*Solanum lycopersicum*) cv Red Cherry (LA0337) was used as the wild-type (WT) for all experiments. Seeds for WT, *af* (LA1049) and the IL5-2 introgression line (LA4055) were obtained from C.M. Rick Tomato Genetics Resource Center (University of California, Davis, CA, USA). Seedlings were grown in Jiffy peat pots (Hummert International) and maintained in a growth chamber as described previously (Chen et al., 2006; Kang et al., 2010b). Three- to four-week-old plants were used for metabolite profiling and analysis of trichome morphology and density.

Metabolite Analysis

For quantification of anthocyanins, leaves from 4-week-old plants were placed in a 2 mL microcentrifuge tube (Dot Scientific) with 1 mL of methanol containing 1% hydrochloric acid and incubated overnight at 4°C. Anthocyanin pigments in the resulting extract were measured spectrophotometrically at 530 nm and 657 nm. Anthocyanin levels were calculated as A530-(0.25A657)/g fresh weight (FW) of leaf tissue (Rabino and Mancinelli, 1986).

Leaves from 4-week-old plants were used to prepare leaf dip or type VI trichome extracts as previously described (Kang et al., 2010b). For analysis of flavonoids and other non-volatile compounds, single leaflets were placed in 1 mL methanol:acetic acid:water (9:1:10) containing 10 µM propyl-4-hydroxybenzoate as an internal standard, and incubated overnight in the dark and with gentle shaking. Alternatively, a defined number of type VI glands, collected with a Pasteur pipette, were dissolved in 100 µL of the same buffer. For analysis of terpenoid compounds, single leaflets were incubated for 5 min (with gentle shaking) in 1 mL methyl *tertiary*-butyl ether (MTBE) containing tetradecane (10 ng μL^{-1}) as an internal standard. Alternatively, type VI glands collected with a Pasteur pipette were dissolved in 100 µL of MTBE containing the internal standard. Quantification of metabolites was performed as described previously, using HPLC/time-of-flight MS for nonvolatile metabolites, and GC-MS for volatiles terpenes (Kang et al., 2010b).

Trichome Density and Morphology

A dissecting microscope (Leica MZ16, Wetzlar, Germany) equipped with KL 2500 LCD light sources (Schott, Germany) and Leica DFC 290 camera (Leica, Germany) was used to document trichome morphology, size, and density. Scanning electron microscopy (SEM) was performed as previously described (Kang et al., 2010b). All measurements were performed on WT and *af* plants grown together in the same growth chamber.

Analysis of Insect Herbivory in Field Plots

Field experiments were performed in the summer of 2008 and 2009. Four-week-old plants grown in the greenhouse were transferred to a test plot on the Department of Plant Pathology Research Farm, Michigan State University (MSU), East Lansing, MI. WT and *af* plants were grown in alternating rows, with 100 cm spacing between plants within and between rows. Plants were watered manually every other day for one week, after which they were allowed to grow under natural conditions. Plants were monitored twice a week for the presence of naturally occurring insect herbivores, as well as for feeding damage by herbivores. Leaf damage inflicted by flea beetle attack was assessed by counting the number of feeding sites (holes) on all leaves of the plant.

Map-Based Cloning of *Af*

Fine mapping of *Af* was performed with an F_2 population derived from a cross between *af* (LA1049) and IL5-2 (LA4055), and was facilitated by the tomato genome sequence (Consortium, 2012). A population of 1255 F_2 plants was scored for the anthocyanin phenotype (AC^+ or AC^-), and subsequently genotyped with PCR-based COS (conserved ortholog set) markers located within the introgressed region of chromosome 5 (Tomato-EXPEN 2000 map; http://solgenomics.net). Fifty-six plants showing recombination between markers C2_At3g25690 and C2_At1g69210 were identified. These recombinants were further genotyped with marker C2_At3g55120, as well as three new markers developed in this region of chromosome 5. Specifically, *S. pennellii* EST sequences generated in the Solanum Trichome Project (http://www.trichome.msu.edu) were used to convert the RFLP markers T1790 and CT93, and the tomato unigene SGN-U564842, to PCR-based markers. Primer sequences used for mapping are listed in Supplemental Table S1. The SGN-U571424 marker is located in the last exon of Solyc05g010300. The C2_At3g55120 marker that cosegregated with the target locus (*CHI1*) is located in the third intron of *CHI1*. Genomic DNA extraction and PCR conditions were as previously described (Kang et al., 2010a).

PCR Analysis

RNA extracted from leaves (Plant RNeasy Kit, Qiagen) was used for cDNA synthesis (Thermoscript RT-PCR system, Invitrogen) according to the manufacturer's protocol. Full-length cDNAs corresponding to *SlCHI1* and *SlCHI2* were amplified by PCR (DNA Engine Dyad Thermal Cycler, Bio-Rad), using the primer set (CHI1 and CHI2) listed in Supplemental Table 2. A cDNA encoding *elongation factor 4A* was PCR-amplified using the elF4A primer (Supplemental Table S2) and used as a loading control. Reverse transcription (RT)-PCR reactions (25-µL) contained 2 µL cDNA, 1 µL of a 10 µM solution of each primer, 0.75 µL of 10 mM dNTP mix, 5 µL of 5X KAPA buffer, and 0.5 µL of KAPA DNA polymerase (KAPAHiFi HotStart, Kapa Biosystems). The amplification protocol included an initial 4-min denaturation step at 95°C, followed by 25 cycles in which the template was denatured for 20 s at 98°C, annealed for 15 s at 52°C, and extended for 40 s at 72°C , followed by a final incubation for 2 min at 72°C. Amplified products were separated on a 1% agarose gel. Full-length genomic DNA corresponding to *SlCHI1* and *SlCHI2* from WT and *af* plants was PCR-amplified using the

primer sets listed in Supplemental Table S2. The PCR-amplified fragments were cloned into the pGEM-T-Easy plasmid vector (Promega). Automated nucleotide sequencing was performed at the Michigan State University Genomics Technology Support Facility (http://rtsf.msu.edu/).

Characterization of Recombinant CHI1

Plasmid pGEM-T containing the *SlCHI1* cDNA isolated from WT or *af* plants was PCR-amplified using the CHI1-NS primer set (Supplemental Table S2). The resulting 0.7-kilobase DNA fragment was digested with *Nde*I and *Sal*I, gel-purified, and ligated into vector pET28b (Novagen) to generate expression constructs pET-CHI1^{WT} and pET-CHI1^{af}, which encode the normal and *af*-mutant forms of CHI1, respectively. These constructs were transformed into *Escherichia coli* strain BL21. A single *E. coli* colony was inoculated into three mL LB medium containing 30 µg mL^{-1} kanamycin, and the culture grown overnight at 37°C. A 100 µL aliquot of this culture was used to inoculate 50 mL LB medium containing 30 µgmL^{-1} kanamycin. The culture was grown to log phase ($A_{600\ nm}$ = 0.4 – 0.8) at 37°C, at which point isopropyl-thio- β -D-galactopyranoside (Sigma-Aldrich) was added to final concentration of 0.5 mM. The culture was grown for an additional 7 h at 20°C. Cells were harvested by centrifugation at 7,000 x *g* and re-suspended in 1 mL lysis buffer containing 50 mM Tris-HCl (pH 8.0), 500 mM NaCl, 20 mM imidazole, 10 mM β-mercaptoethanol, 10% (v/v) glycerol, and 1% (v/v) Tween 20. After sonication and centrifugation, the cleared lysate was applied to a Ni-affinity column (Ni-NTA resin). The column was washed with three column volumes of lysis buffer, followed by a final wash with lysis buffer containing 35 mM imidazole. CHI1-His protein was eluted from the column with lysis buffer containing 250 mM imidazole but lacking Tween 20. Fractions containing CHI1 were pooled and buffer-exchanged to 5 mM HEPES (pH 5.5), 25 mM NaCl, and 1 mM D/L-dithiothreitol with an Amicon Ultra-15 10-kD filter (Millipore). Purified CHI1 proteins were quantified with Pierce® BCA Protein Assay Kit (Thermo Scientific) according to the manufacturer's instructions. Purified recombinant CHI1 enzymes were determined to be >95% pure as determined by SDS-PAGE.

The enzymatic activity of recombinant CHI1 was measured spectrophotometrically as previously described (Jez and Noel, 2002). Briefly, 1 mL reactions containing 100 µM naringenin chalcone, 50 mM HEPES (pH 5.5), 5% (v/v) ethanol, and a known amount of purified CHI1 were incubated at 25°C. The pH was optimized to minimize spontaneous

conversion of naringenin chalcone to naringenin. Naringenin chalcone was purchased from ChromaDex (USA). The time-dependent decrease in absorbance at 360 nm of reactions containing or not containing CHI1 was monitored with a Du® 800 spectrophotometer (Beckman Coulter). Absorbance values recorded in the absence of enzyme were subtracted from values recorded in the presence of CHI1. The time-dependent decrease in absorbance at 360 nm of reactions containing or not containing CHI1 was monitored with a DU® 800 spectrophotometer (Beckman Coulter). Absorbance values recorded in the absence of enzyme were subtracted from values recorded in the presence of CHI1.

Antibody Production and Western-Blot Analysis

Total leaf protein was extracted with buffer containing 100 mM Tris-HCl (pH 6.8), 20 mM EDTA, 100 mM KCl, 1 mM PMSF, and 2% (v/v) 2-mercaptoethanol as described (Chen et al., 2007; Gonzales-Vigil et al., 2011). Rabbit polyclonal antibodies raised against SlCHI1 were obtained from a commercial vendor (Cocalico Biologicals). Purified recombinant SlCHI1 (0.5 mg protein) was used the antigen, according to vendor's standard protocol. Western-blot analysis was performed as previously described (Schilmiller et al., 2007). Anti-CHI1 antibodies were diluted 1:5,000 in TTBS buffer [50 mM Tris (pH 7.4), 500 mM NaCl, 0.05% Tween 20] containing 1% nonfat milk. Blots were washed three times with TTBS buffer and then incubated with a peroxidase-conjugated donkey anti-rabbit secondary antibody (1:15,000 dilution; Thermo Scientific). CHI1 protein-antibody complexes were visualized with the SuperSignal® West Pico chemiluminescent substrate (Thermo Scientific) according to the manufacturer's instructions.

Naringenin Treatment

Naringenin (Sigma) was supplied to *af* seedlings through their cut stem as previously described (Howe et al., 1996). Briefly, three-week-old seedlings grown under standard conditions were excised at the base of the stem with a razor. The cut end of the stem was placed immediately into a 50 ml conical tube containing a solution of 0.1 mM naringenin (dissolved in 0.6% ethanol). Control *af* seedlings were placed into a solution (0.6% ethanol) lacking naringenin. Seedlings were incubated in this condition for 3 d prior to photographing leaves.

Transgenic Plants

Plasmid pGEM-T containing a *SlCHI1* genomic clone was reamplified with CHI1-XS primer set (Supplemental Table S2). The resulting fragment was digested with *Xba*I and *Sac*I to release a 2.4-kb fragment that was cloned into *Xba*I and *Sac*I sites of the pBI-TS binary vector, which contains the Cauliflower Mosaic Virus (CaMV) 35S promoter and nopaline synthase (NOS) terminator (Koo et al., 2006; Schilmiller et al., 2007), to generate pBI-*35S::CHI1*. The *CHI1* promoter region (~1.5 kb) was amplified from a tomato BAC clone (LE-HBa0147F10) by PCR (KAPAHiFi HotStart, Kapa Biosystems), using the CHI1Pro-SX primer set (Supplemental Table S2). The resulting fragment was digested with *Sbf*I and *Xba*I and cloned into *Sbf*I and *Xba*I sites of pBI-*35S::CHI1* to replace 35S promoter. The resulting construct (pBI-*CHI1::CHI1*) was introduced into *Agrobacterium tumefaciens* strain AGLO and used to transform *af* cotyledon explants as described previously (Li et al., 2003; Li et al., 2004). The presence of the T-DNA insert in independent primary (T_0) transformants was confirmed by PCR using M13R-CHI1Pro primer set (Supplemental Table S2) to amplify a fragment spanning the pBI-TS vector sequence and *CHI1* promoter region. Regenerated T_0 transgenic plants containing the *CHI1::CHI1* transgene were potted in soil and transferred to a growth chamber for preliminary biochemical analyses. These plants were subsequently transferred to a greenhouse for collection of seed (T_1 generation) from individual lines. T_1 seedlings exhibiting an AC^+ phenotype were selected from lines in which the ratio of AC^+:AC^- was 3:1. These AC^+ plants were grown in a greenhouse for collection of T_2 generation seed. Lines in which all T_2 progeny exhibited the AC^+ phenotype were selected as being homozygous for the transgene.

Supplemental Material

The following materials are available in the online version of this article.

Supplemental Figure 1. RT-PCR for *CHI1* and *CHI2* from WT and *af* leaves.

Supplemental Figure 2. Affinity purification of $CHI1^{WT}$ and $CHI1^{af}$ expressed in *E. coli*.

Supplemental Figure 3. β-phellandrene levels in F_1 and F_2 plants derived from a cross between the *af* mutant (LA1049) and its reported WT parent (cv Red Cherry, LA0337).

Supplemental Figure 4. Terpenoid accumulation on the leaf surface of *CHI1::CHI1* transgenic lines.

Supplemental Figure 5. Phylogenetic tree of CHI and CHI-fold proteins from cultivated tomato.

Supplemental Figure 6. Amino acid sequence alignment of CHIs from several plant species.

Supplemental Table S1. Description of PCR-based markers for genetic mapping.

Supplemental Table S2. Description of oligonucleotide primers used for PCR.

ACKNOWLEDGEMENTS

We wish to thank Eric Czuprenski and Razi Shaha for assistance with plant growth and genetic mapping experiments, and Dr. Cornelius Barry for helpful advice with genetic mapping. We also acknowledge Ray Hammerschmidt and Gary Zehr for providing field space, the MSU Center for Advanced Microscopy for assistance with SEM, the MSU Mass Spectrometry and Metabolomics Core for GC-MS resources, the SOL Genomics Network (SGN) for BAC clones and bioinformatics resources, and the C.M. Rick Tomato Genetics Resource Center (University of California at Davis) for kindly providing tomato seed stocks.

LITERATURE CITED

Affek HP, Yakir D (2002) Protection by isoprene against singlet oxygen in leaves. Plant Physiol **129:** 269-277

Aziz N, Paiva NL, May GD, Dixon RA (2005) Transcriptome analysis of alfalfa glandular trichomes. Planta **221:** 28-38

Bednar RA, Hadcock JR (1988) Purification and characterization of chalcone isomerase from soybeans. J Biol Chem **263:** 9582-9588

Bedon F, Bomal C, Caron S, Levasseur C, Boyle B, Mansfield SD, Schmidt A, Gershenzon J, Grima-Pettenati J, Seguin A, MacKay J (2010) Subgroup 4 R2R3-MYBs in conifer trees: gene family expansion and contribution to the isoprenoid- and flavonoid-oriented responses. J Exp Bot **61:** 3847-3864

Ben Zvi MM, Shklarman E, Masci T, Kalev H, Debener T, Shafir S, Ovadis M, Vainstein A (2012) PAP1 transcription factor enhances production of phenylpropanoid and terpenoid scent compounds in rose flowers. New Phytol **195:** 335-345

Bleeker PM, Mirabella R, Diergaarde PJ, VanDoorn A, Tissier A, Kant MR, Prins M, de Vos M, Haring MA, Schuurink RC (2012) Improved herbivore resistance in cultivated tomato with the sesquiterpene biosynthetic pathway from a wild relative. Proc Natl Acad Sci USA **109:** 20124-20129

Bohlmann J, Keeling CI (2008) Terpenoid biomaterials. Plant J **54:** 656-669

Boughton AJ, Hoover K, Felton GW (2005) Methyl jasmonate application induces increased densities of glandular trichomes on tomato, *Lycopersicon esculentum.* J Chem Ecol **31:** 2211-2216

Burbulis IE, Winkel-Shirley B (1999) Interactions among enzymes of the Arabidopsis flavonoid biosynthetic pathway. Proc Natl Acad Sci U S A **96:** 12929-12934

Burdick A (1958) New mutants. Tomato Genetics Cooperative Report **8:** 9-11

Chatzopoulou FM, Makris AM, Argiriou A, Degenhardt J, Kanellis AK (2010) EST analysis and annotation of transcripts derived from a trichome-specific cDNA library from *Salvia fruticosa*. Plant Cell Rep **29:** 523-534

Chen H, Gonzales-Vigil E, Wilkerson CG, Howe GA (2007) Stability of plant defense proteins in the gut of insect herbivores. Plant Physiol **143:** 1954-1967

Chen H, Jones AD, Howe GA (2006) Constitutive activation of the jasmonate signaling pathway enhances the production of secondary metabolites in tomato. FEBS Lett **580:** 2540-2546

Clay NK, Adio AM, Denoux C, Jander G, Ausubel FM (2009) Glucosinolate metabolites required for an Arabidopsis innate immune response. Science **323:** 95-101

Dai XB, Wang GD, Yang DS, Tang YH, Broun P, Marks MD, Sumner LW, Dixon RA, Zhao PX (2010) TrichOME: A comparative omics database for plant trichomes. Plant Physiol **152:** 44-54

De Jong WS, Eannetta NT, De Jong DM, Bodis M (2004) Candidate gene analysis of anthocyanin pigmentation loci in the Solanaceae. Theor Appl Genet **108:** 423-432

Dillard CJ, German JB (2000) Phytochemicals: nutraceuticals and human health. J Sci Food Agric **80:** 1744-1756

Dixon RA, Paiva NL (1995) Stress-induced phenylpropanoid metabolism. Plant Cell **7:** 1085-1097

Dixon RA, Xie DY, Sharma SB (2005) Proanthocyanidins - a final frontier in flavonoid research? New Phytol **165:** 9-28

Dudareva N, Martin D, Kish CM, Kolosova N, Gorenstein N, Faldt J, Miller B, Bohlmann J (2003) (E)-beta-ocimene and myrcene synthase genes of floral scent biosynthesis in snapdragon: function and expression of three terpene synthase genes of a new terpene synthase subfamily. Plant Cell **15:** 1227-1241

Dudareva N, Murfitt LM, Mann CJ, Gorenstein N, Kolosova N, Kish CM, Bonham C, Wood K (2000) Developmental regulation of methyl benzoate biosynthesis and emission in snapdragon flowers. Plant Cell **12:** 949-961

Dudareva N, Negre F, Nagegowda DA, Orlova I (2006) Plant volatiles: Recent advances and future perspectives. Crit Rev Plant Sci **25:** 417-440

Duffey SS, Isman MB (1981) Inhibition of insect larval growth by phenolics in glandular trichomes of tomato leaves. Experientia **37:** 574-576

Eshed Y, Zamir D (1995) An introgression line population of *Lycopersicon pennelli* in the cultivated tomato enables the identification and fine mapping of yield-associated QTL. Genetics **141:** 1147-1162

Gonzales-Vigil E, Bianchetti C, Phillips GN, Howe GA (2011) Adaptive evolution of threonine deaminase in plant defense against insect herbivores. Proc Natl Acad Sci USA **108:** 5897-5902

Grotewold E (2006) The genetics and biochemistry of floral pigments. Annu Rev Plant Biol **57:** 761-780

Hirsch AM, Bauer WD, Bird DM, Cullimore J, Tyler B, Yoder JI (2003) Molecular signals and receptors: Controlling rhizosphere interactions between plants and other organisms. Ecology **84:** 858-868

Howe GA, Jander G (2008) Plant immunity to insect herbivores. Annu Rev Plant Biol **59**: 41-66

Howe GA, Lightner J, Browse J, Ryan CA (1996) An octadecanoid pathway mutant (JL5) of tomato is compromised in signaling for defense against insect attack. Plant Cell **8:** 2067-2077

Jander J, Clay N (2011) New synthesis -- Plant defense signaling: New opportunities for studying chemical diversity. J Chem Ecol **37:** 429

Jez JM, Bowman ME, Dixon RA, Noel JP (2000) Structure and mechanism of the evolutionarily unique plant enzyme chalcone isomerase. Nat Struc Biol **7:** 786-791

Jez JM, Noel JP (2002) Reaction mechanism of chalcone isomerase - pH dependence, diffusion control, and product binding differences. J Biol Chem **277:** 1361-1369

Kang JH, Liu GH, Shi F, Jones AD, Beaudry RM, Howe GA (2010a) The tomato *odorless-2* mutant is defective in trichome-based production of diverse specialized metabolites and broad-spectrum resistance to insect herbivores. Plant Physiol **154:** 262-272

Kang JH, Shi F, Jones AD, Marks MD, Howe GA (2010b) Distortion of trichome morphology by the hairless mutation of tomato affects leaf surface chemistry. J Exp Bot **61:** 1053-1064

Kennedy GG (2003) Tomato, pests, parasitoids, and predators: Tritrophic interactions involving the genus *Lycopersicon*. Annu Rev Entomol **48:** 51-72

Kliebenstein DJ (2013) Making new molecules--evolution of structures for novel metabolites in plants. Curr Opin Plant Biol **16:** 112-117

Koo AJK, Chung HS, Kobayashi Y, Howe GA (2006) Identification of a peroxisomal acyl-activating enzyme involved in the biosynthesis of jasmonic acid in Arabidopsis. J Biol Chem **281:** 33511-33520

Lange BM, Wildung MR, Stauber EJ, Sanchez C, Pouchnik D, Croteau R (2000) Probing essential oil biosynthesis and secretion by functional evaluation of expressed sequence tags from mint glandular trichomes. Proc Natl Acad Sci USA **97:** 2934-2939

Li C, Liu G, Xu C, Lee GI, Bauer P, Ling HQ, Ganal MW, Howe GA (2003) The tomato suppressor of prosystemin-mediated responses2 gene encodes a fatty acid desaturase required for the biosynthesis of jasmonic acid and the production of a systemic wound signal for defense gene expression. Plant Cell **15:** 1646-1661

Li JY, Oulee TM, Raba R, Amundson RG, Last RL (1993) Arabidopsis flavonoid mutants are hypersensitive to UV-B irradiation. Plant Cell **5:** 171-179

Li L, Zhao Y, McCaig BC, Wingerd BA, Wang J, Whalon ME, Pichersky E, Howe GA (2004) The tomato homolog of CORONATINE-INSENSITIVE1 is required for the maternal control of seed maturation, jasmonate-signaled defense responses, and glandular trichome development. Plant Cell **16:** 126-143

McDowell ET, Kapteyn J, Schmidt A, Li C, Kang JH, Descour A, Shi F, Larson M, Schilmiller A, An LL, Jones AD, Pichersky E, Soderlund CA, Gang DR (2011) Comparative functional genomic analysis of Solanum glandular trichome types. Plant Physiol **155:** 524-539

Meinke DW (2013) A survey of dominant mutations in *Arabidopsis thaliana*. Trends Plant Sci **18:** 84-91

Middleton E, Kandaswami C, Theoharides TC (2000) The effects of plant flavonoids on mammalian cells: Implications for inflammation, heart disease, and cancer. Pharm Rev **52:** 673-751

Muir SR, Collins GJ, Robinson S, Hughes S, Bovy A, De Vos CHR, van Tunen AJ, Verhoeyen ME (2001) Overexpression of petunia chalcone isomerase in tomato results in fruit containing increased levels of flavonols. Nat Biotech **19:** 470-474

Nagel J, Culley LK, Lu YP, Liu EW, Matthews PD, Stevens JF, Page JE (2008) EST analysis of hop glandular trichomes identifies an O-methyltransferase that catalyzes the biosynthesis of xanthohumol. Plant Cell **20:** 186-200

Ngaki MN, Louie GV, Philippe RN, Manning G, Pojer F, Bowman ME, Li L, Larsen E, Wurtele ES, Noel JP (2012) Evolution of the chalcone-isomerase fold from fatty-acid binding to stereospecific catalysis. Nature **485:** 530-U147

Patra B, Schluttenhofer C, Wu Y, Pattanaik S, Yuan L (2013) Transcriptional regulation of secondary metabolite biosynthesis in plants. Biochim Biophys Acta **1829:** 1236-1247

Peer WA, Murphy AS (2007) Flavonoids and auxin transport: modulators or regulators? Trends Plant Sci **12:** 556-563

Peiffer M, Tooker JF, Luthe DS, Felton GW (2009) Plants on early alert: glandular trichomes as sensors for insect herbivores. New Phytol **184:** 644-656

Pourcel L, Irani NG, Koo AJK, Bohorquez-Restrepo A, Howe GA, Grotewold E (2013) A chemical complementation approach reveals genes and interactions of flavonoids with other pathways. Plant J **74:** 383-397

Rabino I, Mancinelli AL (1986) Light, temperature, and anthocyanin production. Plant Physiol **81:** 922-924

Rasmann S, Kollner TG, Degenhardt J, Hiltpold I, Toepfer S, Kuhlmann U, Gershenzon J, Turlings TCJ (2005) Recruitment of entomopathogenic nematodes by insect-damaged maize roots. Nature **434:** 732-737

Rick CM, Quiros CF, Lange WH, Stevens MA (1976) Monogenic control of resistance in tomato to tobacco flea beetle: Probable repellence by floiar volatiles. Euphytica **25:** 521-530

Ringli C, Bigler L, Kuhn BM, Leiber RM, Diet A, Santelia D, Frey B, Pollmann S, Klein M (2008) The modified flavonol glycosylation profile in the Arabidopsis *rol1* mutants results in alterations in plant growth and cell shape formation. Plant Cell **20:** 1470-1481

Sahu NK, Balbhadra SS, Choudhary J, Kohli DV (2012) Exploring pharmacological significance of chalcone scaffold: A review. Curr Med Chem **19:** 209-225

Sallaud C, Rontein D, Onillon S, Jabes F, Duffe P, Giacalone C, Thoraval S, Escoffier C, Herbette G, Leonhardt N, Causse M, Tissier A (2009) A novel pathway for sesquiterpene biosynthesis from Z,Z-farnesyl pyrophosphate in the wild tomato *Solanum habrochaites*. Plant Cell **21:** 301-317

Saslowsky DE, Warek U, Winkel BS (2005) Nuclear localization of flavonoid enzymes in Arabidopsis. J Biol Chem **280:** 23735-23740

Schilmiller AL, Koo AJK, Howe GA (2007) Functional diversification of acyl-CoA oxidases in jasmonic acid biosynthesis and action. Plant Physiol **143:** 812-824

Schilmiller AL, Last RL, Pichersky E (2008) Harnessing plant trichome biochemistry for the production of useful compounds. Plant J **54:** 702-711

Schilmiller AL, Miner DP, Larson M, McDowell E, Gang DR, Wilkerson C, Last RL (2010) Studies of a biochemical factory: Tomato trichome deep expressed sequence tag sequencing and proteomics. Plant Physiol **153:** 1212-1223

Schilmiller AL, Schauvinhold I, Larson M, Xu R, Charbonneau AL, Schmidt A, Wilkerson C, Last RL, Pichersky E (2009) Monoterpenes in the glandular trichomes of tomato are synthesized from a neryl diphosphate precursor rather than geranyl diphosphate. Proc Natl Acad Sci USA **106:** 10865-10870

Schilmiller AL, Stout J, Weng JK, Humphreys J, Ruegger MO, Chapple C (2009) Mutations in the cinnamate 4-hydroxylase gene impact metabolism, growth and development in Arabidopsis. Plant J **60:** 771-782

Sharkey TD, Singsaas EL (1995) Why plants emit isoprene. Nature **374:** 769-769

Shen GA, Huhman D, Lei ZT, Snyder J, Sumner LW, Dixon RA (2012) Characterization of an isoflavonoid-specific prenyltransferase from *Lupinus albus*. Plant Physiol **159:** 70-80

Stam JM, Kroes A, Li Y, Gols R, van Loon JJ, Poelman EH, Dicke M (2014) Plant interactions with multiple insect herbivores: From community to genes. Annu Rev Plant Biol **65:** in press.

Stergachis AB, Haugen E, Shafer A, Fu W, Vernot B, Reynolds A, Raubitschek A, Ziegler S, LeProust EM, Akey JM, Stamatoyannopoulos JA (2013) Exonic transcription factor binding directs codon choice and affects protein evolution. Science **342:** 1367-1372

Tanksley SD, Ganal MW, Prince JP, Devicente MC, Bonierbale MW, Broun P, Fulton TM, Giovannoni JJ, Grandillo S, Martin GB, Messeguer R, Miller JC, Miller L, Paterson AH, Pineda O, Roder MS, Wing RA, Wu W, Young ND (1992) High-density molecular linkage maps of the tomato and potato genomes. Genetics **132:** 1141-1160

Taylor LP, Grotewold E (2005) Flavonoids as developmental regulators. Curr Opin Plant Biol **8:** 317-323

Tomato Genome Consortium (2012) The tomato genome sequence provides insights into fleshy fruit evolution. Nature **485:** 635-641

Tian D, Tooker J, Peiffer M, Chung SH, Felton GW (2012) Role of trichomes in defense against herbivores: comparison of herbivore response to *woolly* and *hairless* trichome mutants in tomato (*Solanum lycopersicum*). Planta **236:** 1053-1066

Tissier A (2012) Glandular trichomes: what comes after expressed sequence tags? Plant J **70:** 51-68

Tohge T, Watanabe M, Hoefgen R, Fernie AR (2013) The evolution of phenylpropanoid metabolism in the green lineage. Crit Rev Biochem Mol Biol **48:** 123-152

van Schie CC, Haring MA, Schuurink RC (2007) Tomato linalool synthase is induced in trichomes by jasmonic acid. Plant Mol Biol **64:** 251-263

Vogt T (2010) Phenylpropanoid biosynthesis. Mol Plant **3:** 2-20

von Wettstein-Knowles P (1967) Mutations affecting anthocyanin synthesis in the tomato. 1. Genetics, histology, and biochemistry. Heredity **60:** 317-346

Voo SS, Grimes HD, Lange BM (2012) Assessing the biosynthetic capabilities of secretory glands in citrus peel. Plant Physiol **159:** 81-94

Wagner GJ (1991) Secreting glandular trichomes - More than just hairs. Plant Physiol **96:** 675-679

Walker AR, Davison PA, Bolognesi-Winfield AC, James CM, Srinivasan N, Blundell TL, Esch JJ, Marks MD, Gray JC (1999) The TRANSPARENT TESTA GLABRA1 locus, which regulates trichome differentiation and anthocyanin biosynthesis in Arabidopsis, encodes a WD40 repeat protein. Plant Cell **11:** 1337-1349

Wang GD, Tian L, Aziz N, Broun P, Dai XB, He J, King A, Zhao PX, Dixon RA (2008) Terpene biosynthesis in glandular trichomes of hop. Plant Physiol **148:** 1254-1266

Wang W, Wang YJ, Zhang Q, Qi Y, Guo DJ (2009) Global characterization of *Artemisia annua* glandular trichome transcriptome using 454 pyrosequencing. BMC Genom **10**

Xiao Y, Wang J, Dehesh K (2013) Review of stress specific organelles-to-nucleus metabolic signal molecules in plants. Plant Sci **212:** 102-107

Xiao YM, Savchenko T, Baidoo EEK, Chehab WE, Hayden DM, Tolstikov V, Corwin JA, Kliebenstein DJ, Keasling JD, Dehesh K (2012) Retrograde signaling by the plastidial metabolite MEcPP regulates expression of nuclear stress-response genes. Cell **149:** 1525-1535

FIGURE LEGENDS

Figure 1. Schematic overview of terpenoid and flavonoid biosynthetic pathways. The names of compounds and select enzymes (italicized) are as follows: ANS, anthocyanidin synthase; CDP-ME, 4-(cytidine 5'-diphospho)-2-C-methyl-D-erythritol; CDP-MEP, 2-phospho-4-(cytidine 5'-diphospho)-2-C-methyl-D-erythritol; CHS, chalcone synthase; CHI, chalcone isomerase; CMK, 4-(cytidine 5'-diphospho)-2-C-methyl-D-erythritol kinase; DAHP, 3-deoxy-D-*arabino*-heptulosonate 7-phosphate; DFR, dihydroflavonol 4-reductase; DMAPP, dimethylallyl diphosphate; DXP, 1-deoxy-D-xylulose 5-phosphate; DXR, DXP reductoisomerase; DXPS, DXP synthase; F3H, flavanone 3-hydroxylase; FLS, flavonol synthase; FPP, farnesyl diphosphate; FPPS, FPP synthase; GPP, geranyl diphosphate; GPPS, GPP synthase; HDR, 4-hydroxy-3-methylbut-2-enyl diphosphate reductase; IPP, isopentenyl diphosphate; MCT, 2-C-methyl-D-erythritol 4-phosphate cytidylyltransferase; MEP, 2-*C*-methyl-D-erythritol 4-phosphate; PAL, phenylalanine ammonia lyase; PEP, phosphoenolpyruvate. Note that although some sesquiterpenes in tomato are synthesized via the MEP pathway (as shown for simplicity; Sallaud et al., 2009), most sesquiterpenes are derived from the cytosolic mevalonate pathway (not shown).

Figure 2. Anthocyanin and trichome phenotypes of the tomato *af* mutant. A and B, Light microscopy image of the abaxial surface of WT (A) and *af* (B) leaves. C and D, Light microscopy image of WT (C) and *af* (D) stems. E and F, Scanning electron micrographs of the adaxial surface of WT (E) and *af* (F) leaves. Representative type I and type VI trichomes are labeled I and VI, respectively. Scale bars represent 1000 µm (A and B), 500 µm in (C and D), and 100 µm in (E and F). Three-week-old plants were used for all experiments.

Figure 3. *af* leaves are deficient in the production of flavonoid-related metabolites. Levels of the indicated secondary metabolites were measured in leaf-dip extracts (A) and isolated type VI glands (B). Each data point represents the mean ± SE of four biological replicates from WT and *af* plants. Asterisks represent significant differences between WT and *af* plants (unpaired *t* test: * $P < 0.05$; ** $P < 0.01$; *** < 0.001). nd, not detected.

Figure 4. Field-grown *af* plants are susceptible to natural populations of insect herbivores. A, Mean (and ± SE) number of flea beetles on WT and *af* plants. The photographic inset shows a flea beetle feeding on the leaf of the *af* mutant. B, Mean (and ± SE) number of flea beetle feeding sites (see inset in A) on each host genotype. Data in A and B were determined for 30 replicate plants per genotype, 9 d after transplantation of seedlings to the field plot. C, Mean (and ± SE) number of Colorado potato beetles (CPB) on each host genotype. Beetles were counted on 18 replicate WT and *af* plants, 40 d after plants were transplanted to the field. The photograph shows a CPB feeding on the *af* mutant. D, Mean (and ± SE) number of blister beetles on each host genotype. Beetles were counted on 11 replicate WT and *af* plants, 30 d after plants were transplanted to the field. The photograph shows a blister beetle feeding on the *af* mutant. Asterisks represent significant differences between WT and *af* (unpaired *t* test: ** $P < 0.01$; *** $P < 0.001$).

Figure 5. The *Af* gene encodes chalcone isomerase. A, Fine genetic mapping of *Af* delimited the target gene to an interval between marker SGN-U571424 and CT93 on chromosome 5. Numbers in parentheses indicate the number of recombination events identified between markers and the target gene. B, Physical map of the region defined by markers SGN-U571424 and C2_At3g55120. Black boxes indicate exons within three predicted genes (arrows). The asterisk denotes the location of the mutation identified in the last exon of *CHI1*. C, WT and *af*-derived nucleotide sequence (upper) encoding the C-terminus of CHI1 and the corresponding deduced amino acid sequence (lower). Stop codons are indicated by bold capital letters and depicted in the predicted amino acid sequence by asterisks. D, Enzymatic activity of $CHI1^{WT}$ and $CHI1^{af}$. Purified recombinant $CHI1^{WT}$ and $CHI1^{af}$ proteins (0.125 µg) were mixed with substrate (naringenin chalcone) and the amount of the substrate was measured spectrophotometrically (A_{340}) at various times thereafter. Control reactions in which enzyme was omitted were performed in parallel and used to correct for non-enzymatic turnover of the substrate. E, Western blot analysis of CHI protein levels in WT and *af* leaves. Crude leaf extract was separated into supernatant (sup.) and pellet fractions by centrifuging at 21,000 x g for 25 min at 4°C. The resulting supernatant (10 µg protein) and a proportional amount of detergent solubilized protein in the pellet fraction was blotted and probed with a polyclonal antibody against tomato CHI1 (upper panel). The PVDF membrane was stained with Coomassie Blue after western blot

analysis (lower panel). Arrows denote CHI1 and the large subunit of Ribulose-1,5-bisphosphate carboxylase oxygenase (RbcL).

Figure 6. Chemical and genetic complementation of the *af* mutant. A, Three-week-old *af* seedlings were supplied through the cut stem with 0.1 mM naringenin (+Nar) or a mock control (Mock). Anthocyanin accumulation in leaf veins was visualized 3 d after treatment. Photographs in the lower panel (scale bar = 1 mm) show a magnified view of images in the upper panel (scale bar = 2 mm). B, Anthocyanin accumulation in *CHI1::CHI1*-complemented transgenic lines. Anthocyanins were extracted from leaf tissue of WT, *af*, four complemented transgenic lines (*CHI1-2*, *CHI1-3*, *CHI1-4*, and *CHI1-9*), and one non-complemented transgenic line (*CHI1-20*). A photograph of the resulting extract is shown above the spectrophotometric quantification of each genotype. C, Western blot analysis of CHI protein levels in *CHI1::CHI1*-complemented transgenic lines. Soluble protein (20 μg) from leaves of the indicated genotype was blotted and probed with a polyclonal antibody against tomato CHI1. RbcL was used as a loading control as described in legend to Fig. 5E.

Figure 7. *af* leaves are deficient in trichome-borne terpenoid production. Levels of the indicated compound were measured in leaf-dip extracts (A) and isolated type VI glands (B). Each data point represents the mean ± SE of four biological replicates from WT and *af* plants. Asterisks represent significant differences between WT and *af* plants (unpaired *t* test: * $P < 0.05$; ** $P < 0.01$; *** < 0.001).

Figure 8. Terpenoid accumulation in type VI glands from *CHI1::CHI1* transgenic lines. A and B, Levels of β-phellandrene (A) and β-caryophyllene (B) were measured in type VI glands isolated from leaves of the indicated genotype. Transgenic lines (T_2 generation) were homozygous for the transgene, and correspond to the same lines described in the legend to Figure 6. Each data point represents the mean ± SE of three independent plants per line. Asterisks represent significant differences between *af* and other genotype plants (unpaired *t* test: ** $P < 0.01$; *** < 0.001).

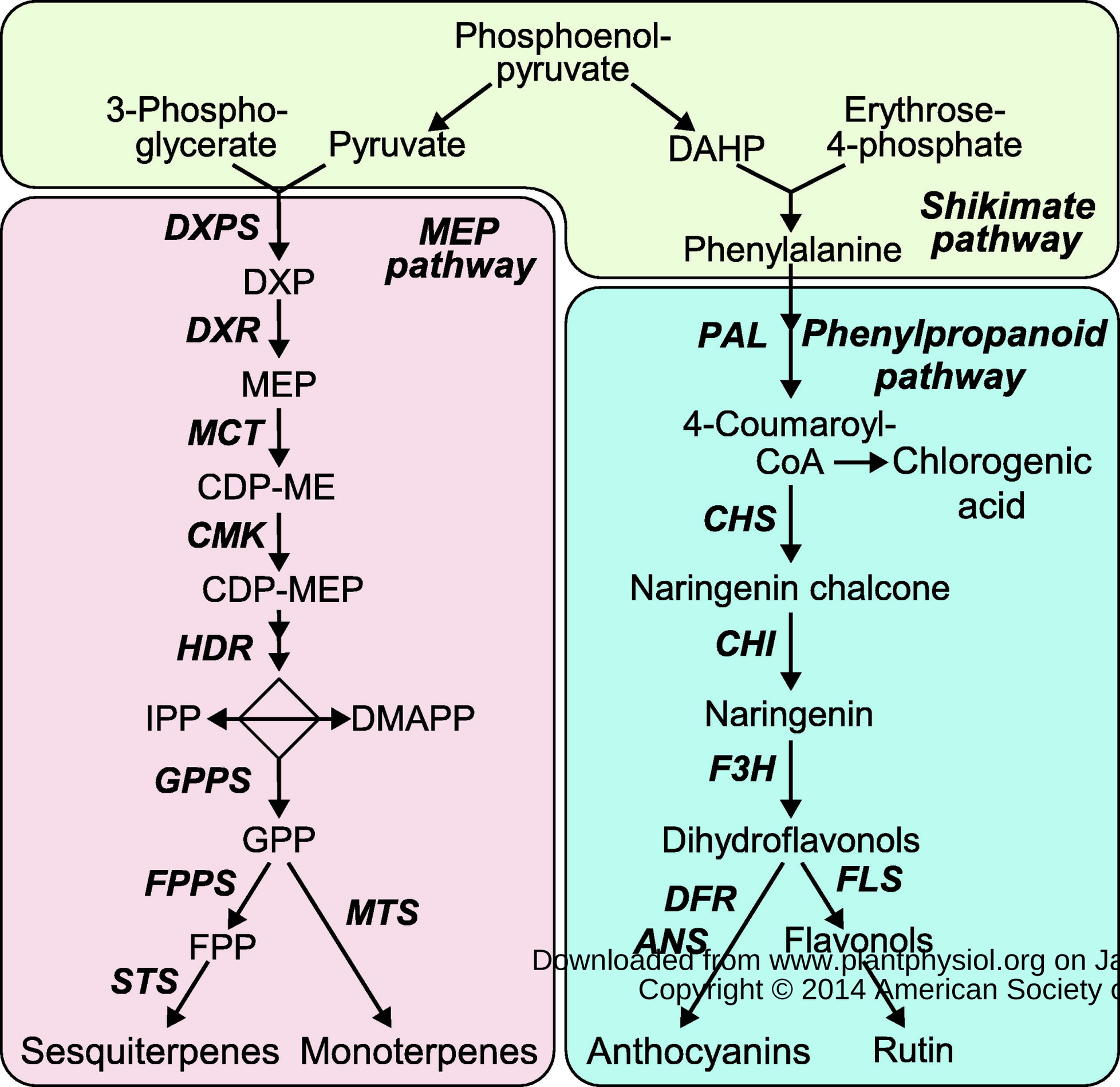

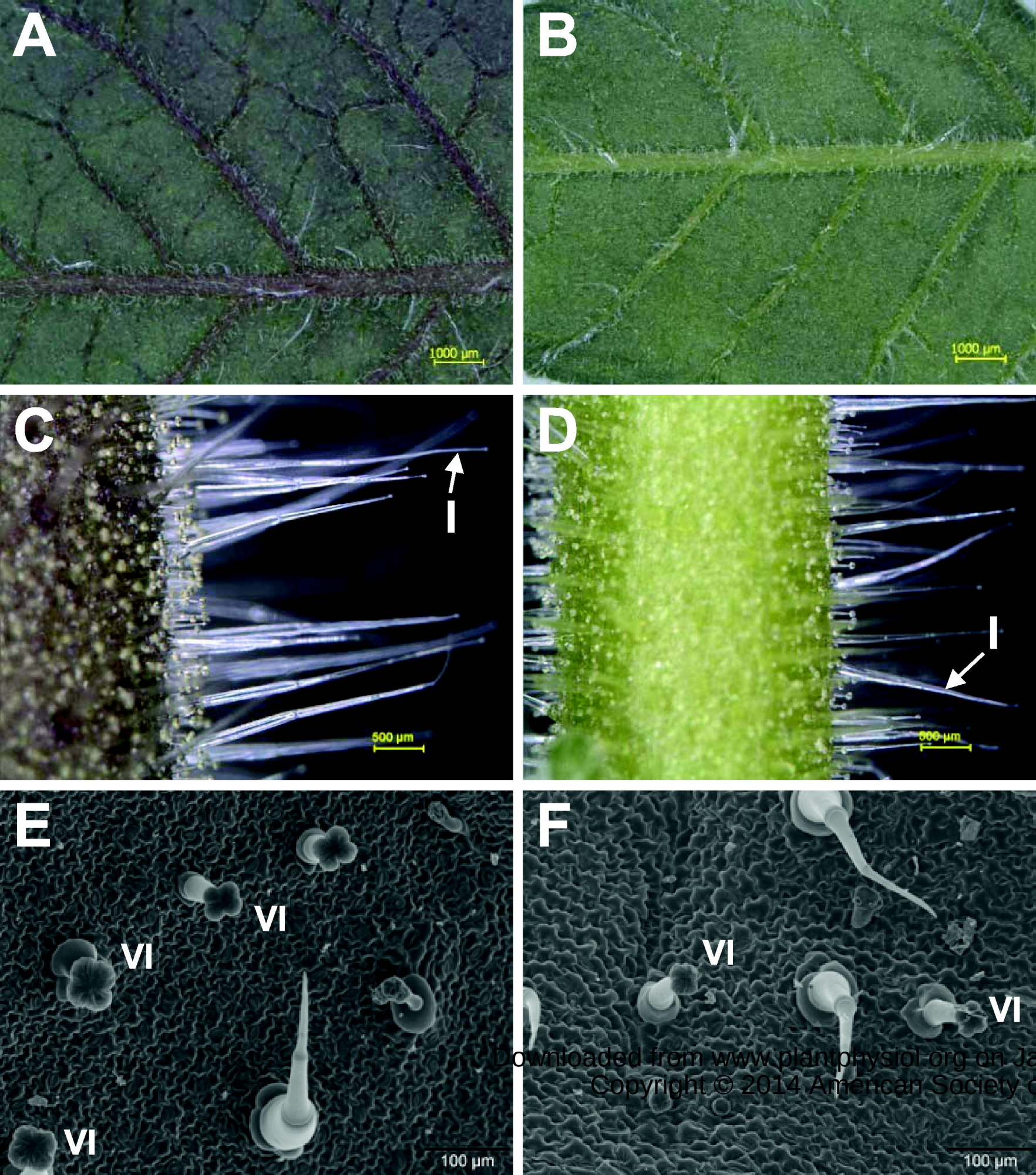

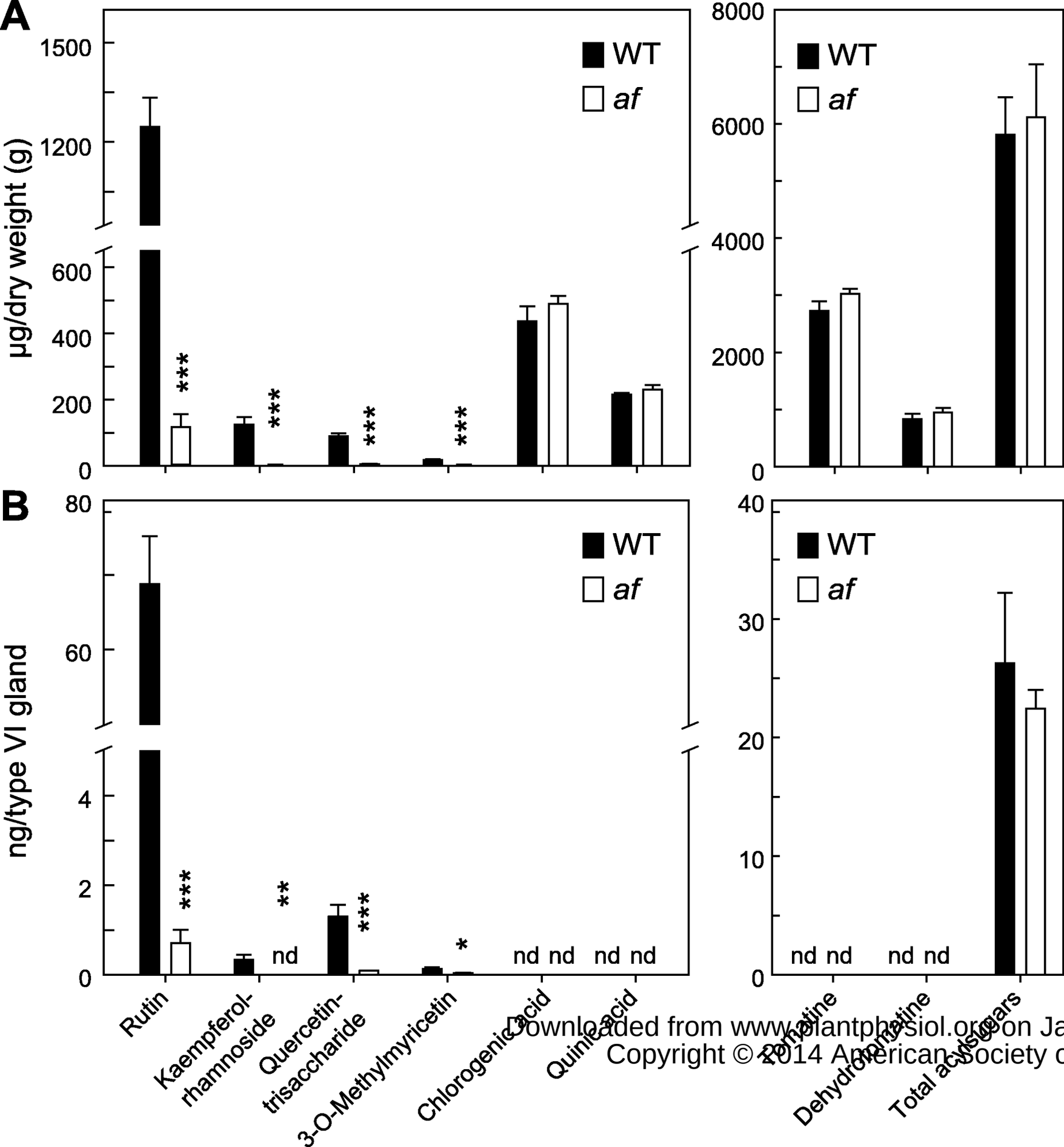

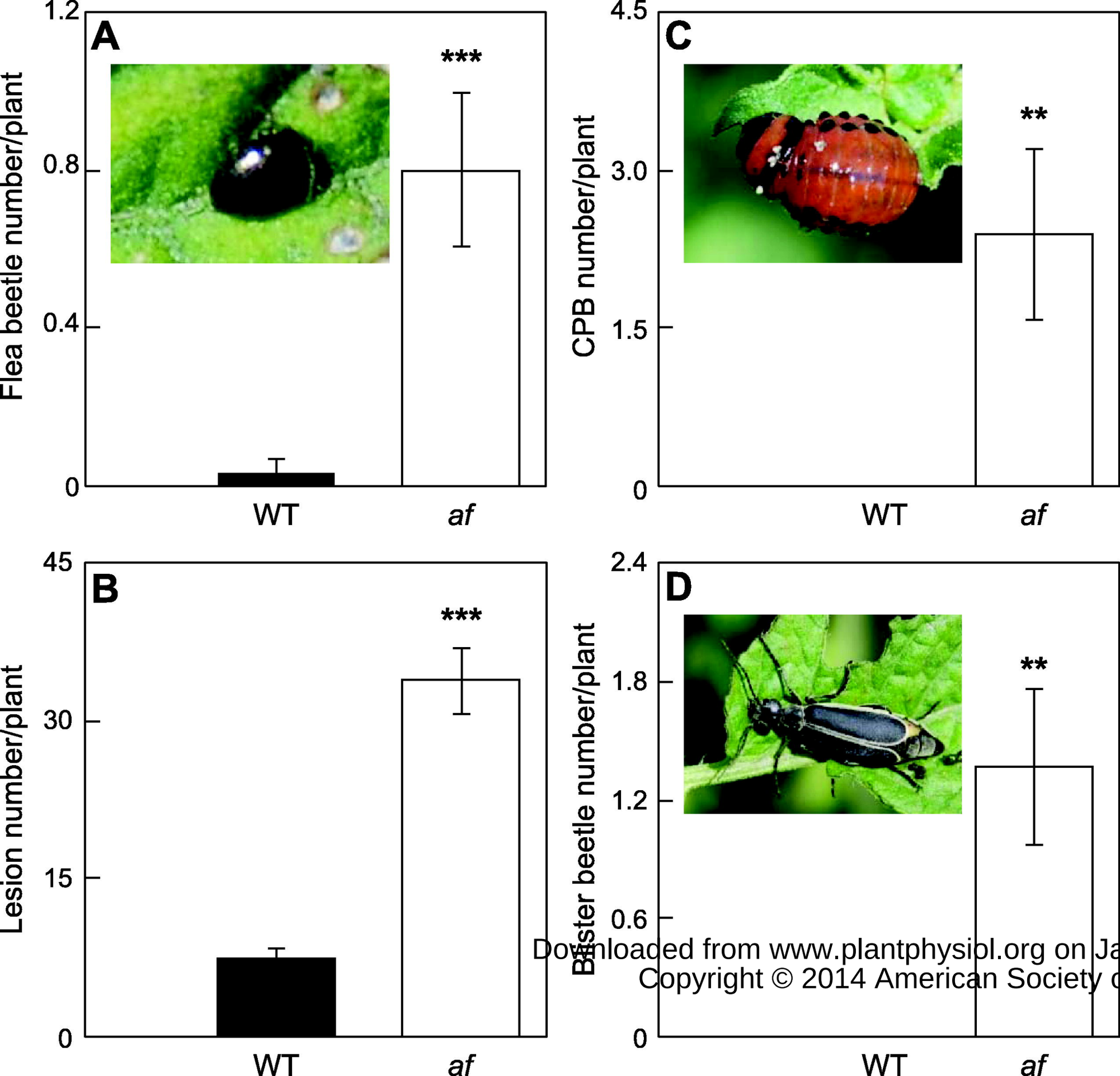

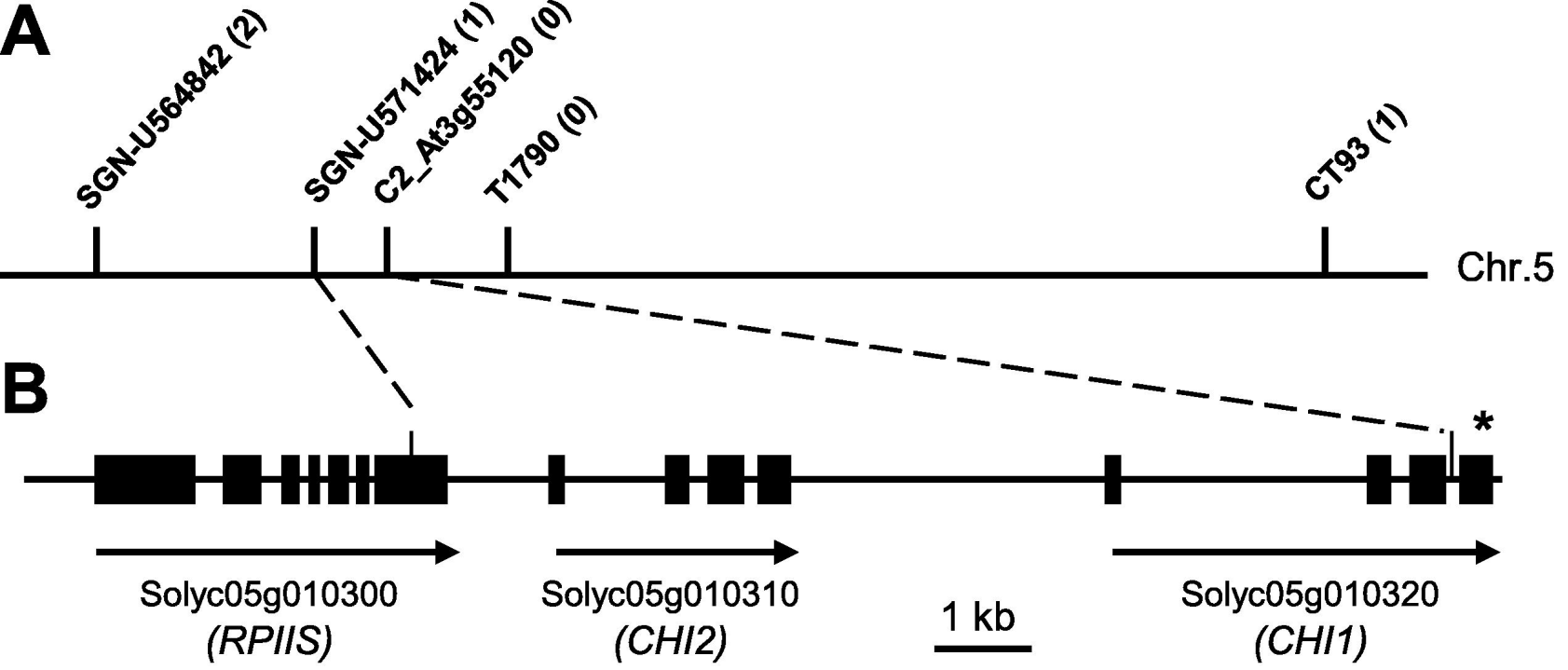

C

```
WT  GCAAAAAGAGTATCAGAACTGTTGGTTTGTGAAAAACCAGGAAGTGAGCTATCGTCAGTCCAG TAA
af  GCAAAAAGAT------AACTGTTGGTTTGTGAAAAACCAGGAAGTGAGCTATCGTCAGTCCAG TAA

WT  A  K  R  V  S  E  L  L  V  C  E  K  P  G  S  E  L  S  S  V  Q  *
af  A  K  R  *
```

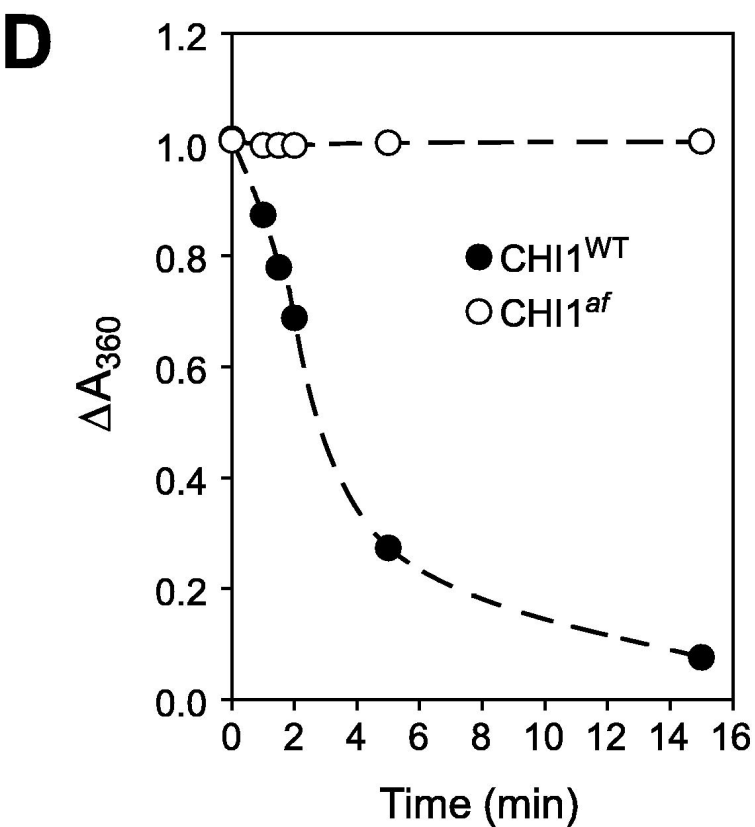

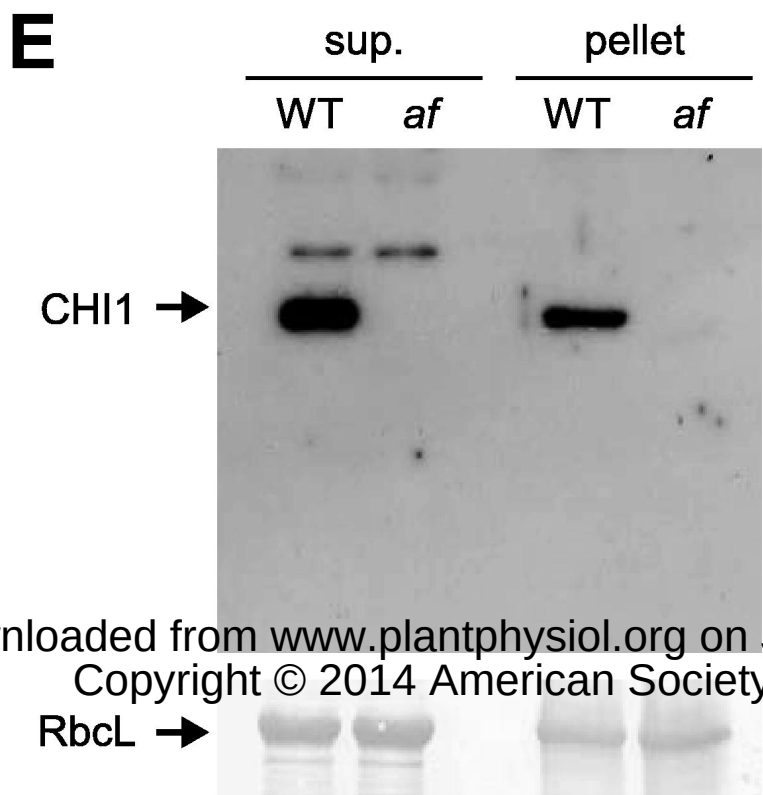

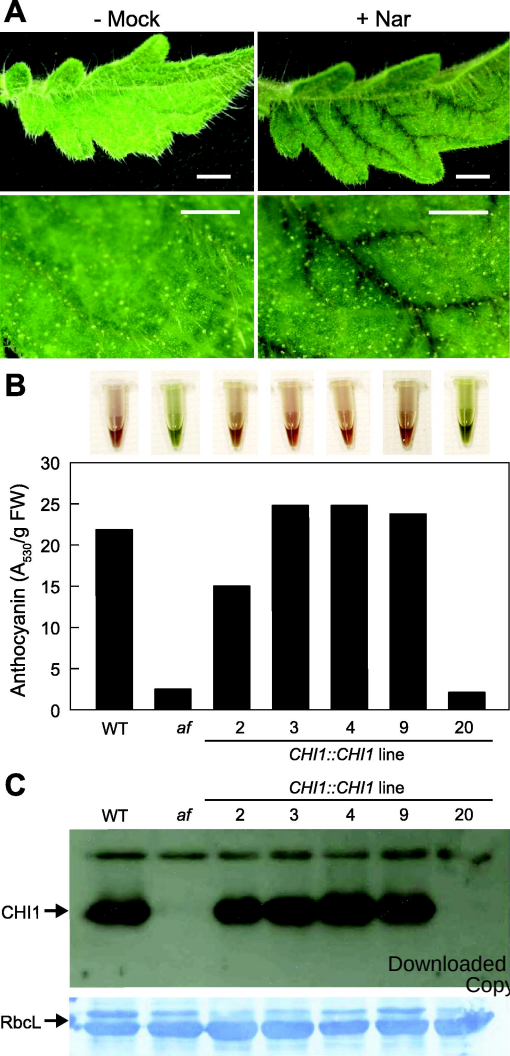
A
- Mock
+ Nar
B
Anthocyanin (A_{530}/g FW)
30
25
20
15
10
5
0
WT
af
2
3
4
9
20
CHI1::CHI1 line
C
CHI1::CHI1 line
WT
af
2
3
4
9
20
CHI1
RbcL
Downloaded
Copy